

Received: 28 March 2011 – Accepted: 10 April 2011 – Published: 15 April 2011

Correspondence to: B. Quennehen (b.quennehen@opgc.univ-bpclermont.fr)

Published by Copernicus Publications on behalf of the European Geosciences Union.

ACPD

11, 11771–11808, 2011

**Physical and
chemical properties
of Arctic aerosols**

B. Quennehen

Title Page

Abstract

Introduction

Conclusions

References

Tables

Figures

⏪

⏩

◀

▶

Back

Close

Full Screen / Esc

Printer-friendly Version

Interactive Discussion



Abstract

Within the framework of the POLARCAT-France campaign, aerosol physical, chemical and optical properties over Greenland were measured onboard the French ATR-42 research aircraft. The Lagrangian particle dispersion model FLEXPART was used to determine air mass origins. The study focuses particularly on the characterization of air masses transported from the North American continent. Air masses that picked up emissions from Canadian and Alaskan boreal forest fires as well as from the cities on the American east coast were identified and selected for a detailed study. Measurements of CO concentrations, aerosol chemical composition, aerosol size distributions, aerosol volatile fractions and aerosol light absorption (mainly from black carbon) are used in order to study the relationship between CO enhancement, ageing of the air masses, aerosol particle concentrations and size distributions. Aerosol size distributions are in good agreement with previous studies, even though, wet scavenging potentially occurred along the pathway between the emission sources and Greenland leading to lower concentrations in the aerosol accumulation mode. The measured aerosol size distributions show a significant enhancement of Aitken mode particles. It is demonstrated that the Aitken mode is largely composed of black carbon, while the accumulation mode is more dominated by organics, as deduced from aerosol mass spectrometric AMS and aerosol volatility measurements. Overall, during the campaign rather small amounts of black carbon from the North American continent were transported towards Greenland. An important finding given the potential climate impacts of black carbon in the Arctic.

1 Introduction

The Polar regions are known to be more strongly impacted by global warming than other regions (IPCC, 2007). Many studies have been carried out to improve our current understanding on climate processes related to short lived climate forcers in the Arctic

Physical and chemical properties of Arctic aerosols

B. Quennehen

Title Page

Abstract

Introduction

Conclusions

References

Tables

Figures

◀

▶

◀

▶

Back

Close

Full Screen / Esc

Printer-friendly Version

Interactive Discussion



**Physical and
chemical properties
of Arctic aerosols**

B. Quennehen

Title Page

Abstract

Introduction

Conclusions

References

Tables

Figures

◀

▶

◀

▶

Back

Close

Full Screen / Esc

Printer-friendly Version

Interactive Discussion



atmosphere (Law and Stohl, 2007), while most of the previous work was based on surface observations (Sirois and Barrie, 1999; Ricard et al., 2002; Quinn et al., 2002, 2008). Few airborne campaigns have been performed to date (Shaw, 1975; Brock et al., 1990; Browell et al., 1992; Dreiling and Friederich, 1997). Furthermore, many advances in measurement techniques, especially for aerosol measurements (aerosol mass spectrometry, aerosol light absorption, aerosol volatility), have been achieved recently (Bond et al., 1999). That is why the POLARCAT (POLar study using Aircraft, Remote sensing, surface measurements and models, of Climate, Chemistry, Aerosols and Transport) project was launched during the 4th International Polar Year (IPY) (2007–2008). POLARCAT's objectives were to increase our knowledge about long range transport of short-lived pollutants (particulates and gases) to the Arctic. The French ATR-42 research aircraft performed 24 scientific flights out of Kiruna, Sweden, in spring (not treated in this study) and twelve flights from Kangerlussuaq, Greenland, in summer 2008. For the campaign, the ATR-42 was equipped with instrumentation measuring the physical, optical, and chemical properties of the aerosols.

Aerosol particles play a major role in global climate change (IPCC, 2007) through direct and indirect effects (Twomey, 1977) on Earth's radiative budget. Especially in the Arctic region, these effects remain poorly investigated and are therefore difficult to quantify, thus implicating large uncertainties (Garrett and Zhao, 2006; Lubin and Vogelmann, 2006). In principle, the Arctic region is characterised by very few pollution sources. However, transport of pollution from outside the Arctic leads to the build up of Arctic Haze, initially observed by pilots flying over Arctic regions (Greenaway, 1950; Mitchell, 1957), and more recently studied by Dreiling and Friederich (1997). A good summary of actual knowledge about aerosols in the Arctic is given in Quinn et al. (2007). The Arctic Haze is composed by a majority of sulphate and particulate organic matter and, to a lower extent, black carbon (Quinn et al., 2002). It originates from forest fires (which are included in the denomination "biomass burning", see the overview by Reid et al., 2005) and/or anthropogenic pollution sources originating from various regions in the Northern Hemisphere like Europe, Siberia, China, or North America.

**Physical and
chemical properties
of Arctic aerosols**

B. Quennehen

[Title Page](#)[Abstract](#)[Introduction](#)[Conclusions](#)[References](#)[Tables](#)[Figures](#)[⏪](#)[⏩](#)[◀](#)[▶](#)[Back](#)[Close](#)[Full Screen / Esc](#)[Printer-friendly Version](#)[Interactive Discussion](#)

While Eckhardt et al. (2003) show that the North Atlantic Oscillation controls air pollution transport to the Arctic, it is not clear yet which source is the largest contributor to the Arctic haze. Stohl (2006), Sharma et al. (2004, 2006) and very recently, in the frame of the ARCPAC campaign, Hirdman et al. (2010), Huang et al. (2010) and Brock et al. (2011) agreed that a major influence stems from the Eurasian sector, including Europe, former USSR, Siberia and Northern China, particularly during the winter and spring seasons. While most recently some efforts have been made to characterise the impact of air masses originating from Eurasia (Sharma et al., 2004, 2006; Stohl, 2006; Stohl et al., 2007; Paris et al., 2009, 2010), long-range transport of North American pollution has been studied to a lesser extent through ice core (McConnell et al., 2007) and model analyses (Hirdman et al., 2010). North American pollution plumes have been studied principally in mid-latitude regions (Honrath et al., 2004; Fiebig et al., 2003; Petzold et al., 2007). During summer, in general Arctic haze does not occur, because of the reduced extent of the polar vortex and significant aerosol removal by wet deposition (Quinn et al., 2007). In summer, boreal fires burning in high-latitude Asia and North America are likely to be more important contributors to Arctic pollution as compared to mid-latitude regions (Stohl et al., 2006; Iziomon et al., 2006; Paris et al., 2009). This study aims to characterise pollution aerosol particles transported to Greenland during the Arctic summer and their consequences for the Arctic climate. After presenting an overview of the ATR-42 instrumentation, analysis of measured chemical and physical aerosol properties (aerosol size distributions, sulphate and organic mass concentrations, aerosol volatility and aerosol absorption) are presented, in order to characterise the composition of Aitken and accumulation modes, related to emission sources and transformation processes during transport.

2 ATR-42 aircraft measurements

During summer 2008 the French research aircraft ATR-42, based in Kangerlussuaq, Greenland performed 12 scientific flights with extensive aerosol measurements. Figure 1 presents all 12 flight tracks. In general, flights performed during the first part of the campaign (on 5, 7 and 8 July) targeted North American air masses, whereas flights on 12, 13 and 14 focused on Siberian fires. Flights on 5 and 7 July were rather clean as compared to the 8 July flight. In addition, North American air masses were also sampled during flights on 12, 13 and 14 July. Since the focus of this study is entirely dedicated to air masses transported from North America, Siberian air masses are not considered here. All pollution plumes (and thus flight periods) discussed in this study, with air masses originating from the North American continent are highlighted in Fig. 1. It is important to notice that the POLARCAT-France flights operating over Southern Greenland may not have sampled Arctic air masses as such but rather air masses on their way into and out of the Arctic, as the Arctic front is typically situated around 70° N in summer (Quinn et al., 2005).

2.1 Physical aerosol properties

Measurements of the aerosol particle size distributions onboard the aircraft were performed using a combination of a Scanning Mobility Particle Sizer (SMPS) described by Villani et al. (2008) and an Optical Particle Counter (OPC, GRIMM model 1.108), both operated inside the aircraft cabin downstream the ATR-42 Community Aerosol Inlet (CAI). The CAI is similar to the one designed for the University of Hawaii by Clarke and described in McNaughton et al. (2007). A Passive Cavity Aerosol Spectrometer Probe (PCASP 100-X, DMT), was operated outside the aircraft fuselage. While the SMPS sizes aerosol particles of diameters in the range $20 < D_p < 500$ nm over 88 channels, the OPC measures in the range $300 < D_p < 2000$ nm over 8 channels, and finally the PCASP in the range $100 < D_p < 3000$ nm over 30 channels. In order to study aerosol particle volatility, another pair of SMPS and OPC instruments (called

Physical and chemical properties of Arctic aerosols

B. Quennehen

Title Page

Abstract

Introduction

Conclusions

References

Tables

Figures

◀

▶

◀

▶

Back

Close

Full Screen / Esc

Printer-friendly Version

Interactive Discussion



hereafter NVSMPS/NVOPC) was operated simultaneously downstream a thermode-
nuder set to 280 °C. Refractory particles recovered after the thermal conditioning are
supposed to be mainly composed of soot, sea salt, mineral dust and the refractory
fraction of organic carbon. The ratio of the volatilized particulate volume (total volume
minus refractory volume) and the total particulate volume is used to retrieve information
about aerosol volatility within the integral size range of SMPS/OPC instruments. Thus,
NVSMPS/NVOPC measurements may be used to estimate the refractory mass assum-
ing this mass to be composed mainly of black carbon with a density of 1.8 g cm⁻³ (Bond
and Bergstrom, 2006; Barnard et al., 2007). Because of possible additional presence
of other refractory compounds, with different particle densities (e.g 2.6 g cm⁻³ for dust
particles), calculated refractory or volatile mass fractions are related to the instrumen-
tal method used in this study. Thus, the conversion into BC mass fractions must be
considered with some caution. In general, a density of 1.7 g cm⁻³ has been used to
determine aerosol particle mass concentrations from the SMPS/OPC size spectra at
ambient temperature.

2.2 Chemical composition and trace gases

The chemical composition of submicron aerosol particles was determined by an Aero-
dyne Time-of-Flight Aerosol Mass Spectrometer (C-ToF-AMS, Schmale et al., 2010).
The AMS instrument samples aerosol through an aerodynamic lens system which fo-
cuses the particle beam onto a vaporizer operated at 600 °C. Before reaching the va-
porizer, the particles pass through a time-of-flight region in a vacuum chamber that al-
lows for particle size determination. The vapour is ionized by 70 eV electrons, and the
generated ions are analysed in a time-of-flight mass spectrometer. For a detailed de-
scription of the C-ToF-AMS see Canagaratna et al. (2007) and Drewnick et al. (2005).
During the POLARCAT-France summer campaign, particulate sulphate and organic
matter were determined for STP (standard temperature and pressure) conditions with
a time resolution of 30 s. The respective detection limits were 0.06 and 0.36 µg m⁻³
on average during the campaign. AMS also measure ammonium, nitrate and chloride

Physical and chemical properties of Arctic aerosols

B. Quennehen

Title Page

Abstract

Introduction

Conclusions

References

Tables

Figures

◀

▶

◀

▶

Back

Close

Full Screen / Esc

Printer-friendly Version

Interactive Discussion



Physical and chemical properties of Arctic aerosols

B. Quennehen

Title Page

Abstract

Introduction

Conclusions

References

Tables

Figures

◀

▶

◀

▶

Back

Close

Full Screen / Esc

Printer-friendly Version

Interactive Discussion



mass concentrations but these are not shown since they were usually below the detection limit. To compensate for the decreasing mass flow into the instrument with increasing altitude a Pressure Controlled Inlet (PCI) was installed upstream the standard AMS inlet system, also guaranteeing isokinetic sampling from the aircraft aerosol inlet (for an extended description of the inlet system and the characterisation of the PCI see Schmale et al., 2010). The specific set-up on the ATR-42 allowed for sampling of particles in the size range between 80 and 800 nm vacuum aerodynamic diameter.

Carbon monoxide (CO) was measured by the MOZART CO analyser instrument, based on the gas filtered correlation principle of infrared absorption by the 4.67 μm fundamental vibration-rotation band of CO and presented in detail by Nédélec et al. (2003). CO is considered here to be a rather inert tracer over timescales of 10–20 days for air masses influenced by combustion processes such as biomass burning and anthropogenic pollution plumes (Forster et al., 2001) at the latitudes considered in this study. Ozone measurements are also available but not discussed here.

2.3 Aerosol optical properties

Beside the instrumentation for physico-chemical analysis of aerosol particles, the ATR-42 was equipped with state of the art instrumentation to measure aerosol optical properties: a Particle Soot Absorption Photometer (PSAP) (Bond et al., 1999) and an aerosol nephelometer (TSI 3563, TSI Inc., St Paul, MN). The PSAP instrument has a detection limit of 10^{-6} m^{-1} for the aerosol light absorption coefficient (σ_{abs}) which can be reduced using the method described by Springston and Sedlacek (2007). An estimation of the absorbing aerosol mass (mass_{abs}) was deduced using the following relationship:

$$\text{mass}_{\text{abs}} = \frac{\sigma_{\text{abs}}}{\sigma_{\text{sp-abs}}} \quad (1)$$

With $\sigma_{\text{sp-abs}}$ the specific absorption coefficient assumed to be $11.6 \text{ m}^2 \text{ g}^{-1}$ (Sharma et al., 2002). The mass of absorbing matter related to the initial detection limit is

90 ng m⁻³. In our case, the PSAP raw transmission signal was smoothed with a 180-second running average, thus decreasing the detection limit to $1.75 \times 10^{-7} \text{ m}^{-1}$, corresponding to a mass of 15 ng m⁻³. Even with this improved detection limit, PSAP measurements are often found to be below or just slightly above the detection limit.

3 Classification of sampled air masses

The Lagrangian particle dispersion model FLEXPART (version 6.2) (Stohl et al., 1998, 2005) was used in a backward mode (Stohl et al., 2003) to characterise the origin of the sampled air masses. The model was initialized for small segments along the flight tracks, i.e., whenever the aircraft position changed more than 0.20° horizontally or 150 m vertically, and air masses were traced 20 days backward in time. Meteorological analyses from the European Center of Medium-Range Weather Forecast (ECMWF) with 0.5 × 0.5° resolution were used to drive the model. The primary output of FLEXPART backward calculations is a potential emission sensitivity (PES). Column-integrated PES values were used here mainly to characterise the origin and transport pathways of the sampled air masses. When multiplying the PES values in the lowest model layer (0–100 m), the so-called footprint, with CO emissions from anthropogenic and fire sources, CO source contribution maps and CO tracer mixing ratios (assuming no loss during the 20-day calculations) at the aircraft location can be calculated. Using the column-integrated PES and the footprint PES, four predominant air mass origins were visually identified for the entire measurement campaign:

1. Europe, corresponding to Iceland, Great Britain, Scandinavia and western Russia,
2. Asia, including Siberia and northern China where many boreal forest fires took place,
3. the Arctic, and
4. North America, representing the closest pollution source region from Greenland.

Physical and chemical properties of Arctic aerosols

B. Quennehen

Title Page

Abstract

Introduction

Conclusions

References

Tables

Figures

◀

▶

◀

▶

Back

Close

Full Screen / Esc

Printer-friendly Version

Interactive Discussion



**Physical and
chemical properties
of Arctic aerosols**B. Quennehen

[Title Page](#)[Abstract](#)[Introduction](#)[Conclusions](#)[References](#)[Tables](#)[Figures](#)[◀](#)[▶](#)[◀](#)[▶](#)[Back](#)[Close](#)[Full Screen / Esc](#)[Printer-friendly Version](#)[Interactive Discussion](#)

This study focuses on air masses originating from North America, and especially from three source regions: (i) Canadian and (ii) Alaskan boreal forest (fires) and, (iii) American anthropogenic pollution. In order to illustrate differences between these three North American origins, Fig. 2 presents the FLEXPART column-integrated PES maps for these origins. Forest fires and fires from other sources (mostly agricultural fires) detected by the satellite-based spectro-radiometer MODIS (Moderate Resolution Imaging Spectro-radiometer) and treated by the algorithms illustrated in Giglio et al. (2003), are represented by red and black dots respectively if the PES value on the day of the fire detection was larger than 8 ns m kg^{-1} .

Polluted North American air masses were encountered during 4 of the 12 scientific flight missions on 8, 12 (PM), 13 and 14 (PM) of July. For these four flights, we identified 16 periods when air masses, according to FLEXPART column-integrated PES, originated from one of these three regions. In more detail, we selected 11 time windows related to Canadian and 3 periods related to Alaskan boreal forest fires, respectively, as well as 2 time windows of American anthropogenic origins.

4 Results and discussions

4.1 Aerosol chemical composition

To characterise the aerosol particle sources, the ratio between particulate organic matter and particulate sulphate abundances can give an indication about the source type. For anthropogenic sources, i.e., fossil fuel combustion from North America, high sulphate concentrations are expected (Heald et al., 2006; Singh et al., 2010; Schmale et al., 2011), whereas large concentrations of organics and low concentration of sulphate are expected for Canadian and Alaskan boreal forest fire sources (Andreae and Merlet, 2001; Schmale et al., 2011). Figure 3 presents stacked time series of the concentrations of sulphate, organics, and NVSMPS/NVOPC derived refractory particulate matter observed during the four flights of interest (ATR-42 flights 8, 12, 13 and

14 July 2008). The 16 time windows for North American air masses are highlighted by three different colours (red for Canadian boreal forest fires, yellow for American pollution and, blue for Alaskan air masses). Periods when the aircraft sampled inside clouds are highlighted in grey and are excluded from the analysis due to sampling errors of the aerosol inlet. All other peaks in the measured mass concentrations are due to air masses from other source regions that are not within the focus of this study. In addition, the total particulate mass estimated from SMPS/OPC measurements at ambient temperature is represented in blue. Since the AMS operated at 600 °C and the NVSMPS/NVOPC at 280 °C, the sum of these two particle mass measurements is expected to be greater than the estimated mass determined by the SMPS/OPC because aerosols evaporating between 280 and 600 °C are accounted for twice. For this calculation only particles with diameters smaller than 500 nm were taken into account. Furthermore, Fig. 4 illustrates averaged concentrations for selected time windows, where air mass origins, according to FLEXPART, are indicated on the x-axis. For air masses from North-American anthropogenic sources (AN) and Canadian boreal forest fires (BF), the chemical compositions agreed well with those expected above, thus, confirming the choice of the time windows, whereas Alaskan air masses (AK) seem to bear boreal forest fires characteristics in two cases but fossil fuel combustion characteristics in the third case.

4.2 CO concentrations

During summer, the tropospheric CO background mixing ratios in the Northern Hemisphere are on the order of 90 ppbv (Real et al., 2007). For the above selected 11 periods of sampled North American air masses, time series of CO mixing ratios and enhanced CO mixing ratios (beyond background) are presented in Fig. 5 and Table 2, respectively. While the North American anthropogenic air masses for the flights on 8 and 12 July seem to be related to higher CO levels, this is less evident for flights on 13 and 14 July where the CO levels for several time windows correspond to non polluted background air. In addition, it is important to note that, during the whole campaign,

Physical and chemical properties of Arctic aerosols

B. Quennehen

Title Page

Abstract

Introduction

Conclusions

References

Tables

Figures

◀

▶

◀

▶

Back

Close

Full Screen / Esc

Printer-friendly Version

Interactive Discussion



CO enhancement never reached very high levels. Using the FLEXPART fire tracer age spectra described in Stohl et al. (2005) as well as the FLEXPART biomass burning potential source contributions (Stohl et al., 2007), the age of each Canadian air mass and the related sources strength were estimated. Mean age values are given in Table 2.

The source contribution (CO_{emi}) is playing an important role in the mean particle concentrations. Since air masses studied here are originated from different sources, the ratio between mean particle concentrations (with diameter lower than 500 nm) and source contributions (called hereafter $\Delta\text{N}/\text{CO}_{\text{emi}}$) is used in the following analyses. The relationship between $\Delta\text{N}/\text{CO}_{\text{emi}}$ and the FLEXPART plume age as well as $\Delta\text{N}/\text{CO}_{\text{emi}}$ and CO enhancements are presented in Fig. 6a and Fig. 6b, respectively. $\Delta\text{N}/\text{CO}_{\text{emi}}$ decrease with ageing of the air mass following an exponential law. This result is in good agreement with findings in Schmale et al. (2011) who presented similar trends of decreasing aerosol mass concentrations as a function of the plume age after emission. However, the correlation between $\Delta\text{N}/\text{CO}_{\text{emi}}$ and CO enhancement is low ($R^2 = 0.23$), probably due to aerosol cloud scavenging. This result is also in agreement with Schmale et al. (2011) who did not find any correlation. In the following section, the possibility of aerosol cloud scavenging on their way to the sampling location is investigated. Variable degrees of scavenging may explain the dispersion of the data points around the exponential fit in Fig. 6a and 6b.

4.3 Aerosol size distributions

To study aerosol physical properties, raw aerosol size distributions measured during the diagnosed time periods were fitted with lognormal distributions. The lognormal fitting method was based on four aerosol particle modes. In contrast to the volatility analysis where we used data from the (V)SMPS and (V)OPC, for the discussion of the aerosol size distributions, we used a combination of SMPS and PCASP instruments to cover the largest possible size range measured during the campaign. SMPS data cover the range $20 < D_p < 500$ nm, and PCASP data the range $500 < D_p < 3000$ nm. The latter was chosen because of its more precise channels compared to the OPC (30 channels

Physical and chemical properties of Arctic aerosols

B. Quennehen

Title Page

Abstract

Introduction

Conclusions

References

Tables

Figures

◀

▶

◀

▶

Back

Close

Full Screen / Esc

Printer-friendly Version

Interactive Discussion



**Physical and
chemical properties
of Arctic aerosols**

B. Quennehen

Title Page

Abstract

Introduction

Conclusions

References

Tables

Figures

◀

▶

◀

▶

Back

Close

Full Screen / Esc

Printer-friendly Version

Interactive Discussion



for the PCASP against 8 for the OPC) and because of its mounting position outside the plane. In principle, because of the aerosol refractive index variability, PCASP data have to be corrected based on the Lorentz-Mie theory (Bohren and Huffman, 1983). Since not enough information is available to precisely determine the complex refractive index along the flight tracks, the PCASP data presented here have not been corrected. Instead particles were treated as latex spheres with a refractive index of 1.59. According to Schwarz et al. (2008) and Hosseini et al. (2010), fresh soot particles from biomass burning and urban pollution are limited in size to diameters below 300 nm. However, soot particles can be coated with other atmospheric components such as organics and sulphate (Bond et al., 2006). Previous studies, (Fiebig et al., 2003; Petzold et al., 2007) showed measurements of aerosol physico-chemical properties, over Germany and Central Europe, of aged North American biomass burning air masses. Both studies highlighted large mean diameters between 200 and 340 nm for the accumulation mode, for air mass ages of 6 to 9 days. In these studies, air mass ages were also estimated using FLEXPART in Petzold et al. (2007) and through a theoretical approach demonstrated by Reid et al. (1998) and used in Fiebig et al. (2003).

Figure 7 presents the raw and fitted aerosol size distributions for air masses originating from North America for each flight considered in this study. In order to fit the raw size distributions, the log-normal parameterisation is working with four modes, instead of only three modes chosen in the studies presented by Fiebig et al. (2003) and Petzold et al. (2007). The fit of four modes was used to yield an improved approximation of the raw data, as compared to using three modes, thus, leading to the introduction of an “intermediate” mode between the Aitken and accumulation modes. The different log-normal parameters (i.e., number concentrations n_i , the standard deviation σ_i , and the mean diameter d_{mi} where i is the mode number) are given in Table 1.

A major result regarding the aerosol size distributions from Canadian boreal forest fires (BF) is that for at least 7 out of 11 plume cases, relatively high Aitken mode particle concentrations are associated to a small average standard deviation of 1.38 and a rather small average mean diameter of 44.1 nm. These values are comparable to the

**Physical and
chemical properties
of Arctic aerosols**

B. Quennehen

[Title Page](#)[Abstract](#)[Introduction](#)[Conclusions](#)[References](#)[Tables](#)[Figures](#)[⏪](#)[⏩](#)[◀](#)[▶](#)[Back](#)[Close](#)[Full Screen / Esc](#)[Printer-friendly Version](#)[Interactive Discussion](#)

parameters reported by Hosseini et al. (2010) who found average size distributions with mean diameters between 25 and 52 nm and with standard deviations between 1.58 and 1.76 in laboratory studies of biomass burning aerosol particles. This would also mean that measured boreal forest fire particles have neither been coated to a significant extent nor coagulated noteworthy during the 7–13 days of transport. Alternatively, coagulation proceeded at a rate proportional to the square of the particle concentration (Hinds, 1999). Since the aerosol number and mass concentrations in North American pollution plumes measured during the POLARCAT campaign are not as high as the ones measured during other campaigns (Petzold et al., 2007; Fiebig et al., 2003), the coagulation process is expected to be slower in plumes studied here, implicating an increased Aitken mode lifetime.

A comparison of aerosol size distributions measured during the above mentioned other studies with those determined within POLARCAT (this study, Fig. 7) is presented in Fig. 8. Concerning the accumulation mode, measured concentrations and mean diameters were lower during POLARCAT than those reported by Fiebig et al. (2003) and Petzold et al. (2007). The differences between the size distributions, principally concerning the accumulation mode concentrations, might be explained by a cleansing of accumulation mode particles due to cloud scavenging. To investigate this, we used the HYSPLIT on-line version of the Lagrangian back-trajectory model (Draxler and Rolph, 2010; Rolph, 2010) that provides, in addition to the back-trajectory coordinates, the relative humidity (RH) along the trajectories. The back-trajectories for 8 July are presented in Fig. 9 where RH, altitude, and the ECMWF total column precipitation are colour coded, respectively. Fire hot spots from MODIS are highlighted by red squares. It appears that almost all 11 air masses containing particles from forest fires experienced relative humidities near 100% coupled to important amounts of precipitation after passing over the fire regions. This leads to the conclusion that in most of the cases, the accumulation mode is likely to have been scavenged by cloud processes.

4.4 Aerosol volatility

The aerosol volatile fraction from SMPS + OPC and NVSMPS + NVOPC data was calculated using the following equation:

$$\text{Volatile fraction} = \frac{V_{\text{ambient}} - V_{280^{\circ}\text{C}}}{V_{\text{ambient}}} \quad (2)$$

5 Where, V_{ambient} and $V_{280^{\circ}\text{C}}$ are corresponding to the aerosol volume at ambient temperature and at 280°C , respectively. Figure 10 presents the mean volatile fractions for the 16 identified plumes. Air masses related to the Canadian boreal forest fires present similar volatility properties, except for the two time windows on 13 July, corresponding to air masses staying 4 days over the Atlantic Ocean before reaching Greenland. Their
10 mean volatile volume fraction is 0.78 ± 0.06 suggesting that the largest particles are mainly composed of sulphate and volatile organics with low vaporisation temperatures, and thus 22% of the particle volume correspond to refractory material. Because of the low absorption coefficients measured by the PSAP for BF aerosol particles, we suggest that the contribution of black carbon to the total aerosol volume is rather low and stems
15 primarily from Aitken mode particles while organics and sulphate, i.e. volatile materials, are important contributors to the total aerosol volume that corresponds principally to the accumulation mode particles. On the one hand, this suggestion is supported by the low values for the absorption coefficient despite the fact that CO (in Fig. 5), as well as sulphate and organics (in Fig. 3) indicate elevated pollution levels. On the other
20 hand, the comparison of SMPS Aitken mode number concentrations and NVSMPS refractory “Aitken” mode illustrates that large fractions of the SMPS measured Aitken mode are detected in the NVSMPS distribution of refractory particles below the detection limit of 20 nm. This indicates that a large fraction of small Aitken mode particles is refractory. In the following section, we relate the high Aitken mode concentrations
25 measured over Greenland to the small amount of absorbing material observed.

Physical and chemical properties of Arctic aerosols

B. Quennehen

Title Page

Abstract

Introduction

Conclusions

References

Tables

Figures

◀

▶

◀

▶

Back

Close

Full Screen / Esc

Printer-friendly Version

Interactive Discussion



4.5 Aerosol absorption properties

As mentioned in Sect. 2.3, PSAP measurements were close to detection limit during the entire POLARCAT summer measurement period. A 180-second running average was applied to smooth the raw transmission data for subsequent calculations of BC contents (volume, mass). The mean absorbing aerosol mass, determined with Eq. (1), is found to be $22.6 \pm 5.9 \text{ ng m}^{-3}$. For comparison reason of aerosol volume from integrated volume size distributions, the absorbing volume (V_{psap}) of particulate matter was calculated from the PSAP absorption coefficient measurements (σ_{abs}) using the following relationship:

$$V_{\text{psap}} = \frac{\sigma_{\text{abs}}}{\rho \cdot \sigma_{\text{sp-abs}}} \quad (3)$$

with $\sigma_{\text{sp-abs}}$ the specific absorption coefficient and ρ the particle density assumed to be $11.6 \text{ m}^2 \text{ g}^{-1}$ (Sharma et al., 2002) and 1.8 g cm^{-3} (Bond and Bergstrom, 2006; Barnard et al., 2007), respectively.

In order to support the above findings that black carbon is mainly associated to the Aitken mode, the absorbing particle volume V_{psap} was compared to the Aitken mode related volume, V_{aitken} deduced from SMPS measurements. V_{aitken} is calculated from fitted size distributions (see Table 1) of Aitken and intermediate modes for diameters lower than 80 nm. These two volumes (V_{psap} and V_{aitken}) for air masses originating from Canadian boreal forest fires, are compared in Table 2. Thus, the ratio (V_{ratio}) between V_{psap} and V_{aitken} gives information about the fraction of BC particles within the Aitken mode. For most of the studied time windows, V_{ratio} yields percentages between 18% and 97% except for one time window where the ratio slightly exceeds 100%. This confirms our idea that, for air masses reaching Greenland from North America during the measurement period, BC is mainly found in the Aitken mode.

Title Page

Abstract

Introduction

Conclusions

References

Tables

Figures

◀

▶

◀

▶

Back

Close

Full Screen / Esc

Printer-friendly Version

Interactive Discussion



5 Conclusions

In this study, we have analysed in-situ aerosol and gas phase measurements performed during the POLARCAT-France summer campaign using the ATR-42 research aircraft based at Kangerlussuaq, Greenland. Measurements of aerosol size distributions, chemical composition, aerosol light absorption coefficient, aerosol refractory properties as well as carbon monoxide concentrations were analysed. FLEXPART Lagrangian simulated backward potential emission sensitivities were used to classify air masses. Time windows with clearly identified North American origins have been used in further analysis. The raw average aerosol number size distributions were fitted assuming four aerosol modes for the time periods. Focusing on the air masses representing Canadian boreal forest fires (BF), the mean aerosol particle concentrations appear to decrease exponentially with respect to plume life time after emission and thus, correlate with the decrease of CO enhancement. However, correlations of particle concentrations with plume age from FLEXPART and CO enhancements show significant scattering of data points, probably due to the scavenging of predominantly accumulation mode particles by clouds during transport from North America to Greenland. Particularly high Aitken particle mode concentrations compared to the accumulation mode concentrations were found. Comparing the fitted number size distributions of this study with results published by Fiebig et al. (2003) and Petzold et al. (2007), important differences were found particularly in the accumulation mode concentrations which may be explained by the different measurement locations and most likely aerosol scavenging via clouds. The accumulation mode is less important as compared to Fiebig et al. (2003) and Petzold et al. (2007) and is mainly composed of sulphate and more volatile organics. Absorbing aerosols, i.e., black carbon, are found to be predominantly contained in the pronounced Aitken mode which is derived mainly from SMPS Aitken mode particles and NVSMPS refractory Aitken mode. The finding is also supported by the fact that despite significant indications of moderate Arctic pollution (higher CO and organic carbon concentrations, variations of aerosol size distributions and FLEXPART

Physical and chemical properties of Arctic aerosols

B. Quennehen

Title Page

Abstract

Introduction

Conclusions

References

Tables

Figures

◀

▶

◀

▶

Back

Close

Full Screen / Esc

Printer-friendly Version

Interactive Discussion



potential emission sensitivity) the light absorption coefficients are very low indicating low BC mass concentrations.

To resume, we finally state that within the observed external mixture, BC is predominantly attributed to the Aitken mode, while organics and sulphate containing particles are more associated to the accumulation mode. Hence pollution from North America contained only small amounts of BC mass and was mainly composed of sulphate and organics during the measurement period of POLARCAT summer. This implicates that in our case no significant amounts of BC mass are transported to Greenland from the North American continent, at least not during the summer observation period. Thus, we state low potential of BC deposition from North America on the Greenland surface ice/snow and therefore, limited impact on the surface albedo during POLARCAT Arctic summer observational period, since observed Aitken mode BC is unlikely to be activated into cloud particles and thus unlikely to be scavenged by Arctic clouds. To answer the question if the above findings for North American pollution plume can be generalised, more measurements and modelling studies are needed in the future.

Acknowledgements. The authors would like to thank the French research agencies ANR, CNES, CNRS-INSU, and IPEV as well as EUFAR. We acknowledge funding by the German Research Foundation (DFG) through the SPP 1294, by the state-“Exzellenzcluster Geocycles” of Rheinland-Pfalz, and by the Max Planck Society. NILU researchers were supported by the Norwegian Research Council in the framework of POLARCAT-Norway and CLIMSLIP. We also would like to thank SAFIRE and Christophe Gourbeyre for their support during the planning and execution of the French ATR-42 campaigns and, together with DT-INSU, for help with instrument integration. Finally, we gratefully acknowledge the NOAA Air Resources Laboratory (ARL) providing the HYSPLIT transport and dispersion model and/or the READY website (<http://www.arl.noaa.gov/ready.php>) used in this publication.

Physical and chemical properties of Arctic aerosols

B. Quennehen

Title Page

Abstract

Introduction

Conclusions

References

Tables

Figures



Back

Close

Full Screen / Esc

Printer-friendly Version

Interactive Discussion



The publication of this article is financed by CNRS-INSU.

References

- Andreae, M. O. and Merlet, P.: Emission of trace gases and aerosols from biomass burning, *Global Biogeochem. Cy.*, 15(4), 955–966, 2001. 11780
- Barnard, J. C., Kassianov, E. I., Ackerman, T. P., Johnson, K., Zuberi, B., Molina, L. T., and Molina, M. J.: Estimation of a “radiatively correct” black carbon specific absorption during the Mexico City Metropolitan Area (MCMA) 2003 field campaign, *Atmos. Chem. Phys.*, 7, 1645–1655, doi:10.5194/acp-7-1645-2007, 2007. 11777, 11786
- Bohren, C. F. and Huffman, D.: *Absorption and scattering of light by small particles*, John Wiley, New York, 1983. 11783
- Bond, T. C., Anderson, T. L., and Campbell, D.: Calibration and intercomparison of filter-based measurements of visible light absorption by aerosols, *Aerosol Sci. Technol.*, 30(6), 582–600, 1999. 11774, 11778
- Bond, T. C. and Bergstrom, R. W.: Light Absorption by Carbonaceous Particles: An Investigative Review, *Aerosol Sci. Technol.*, 40(1), 27–67, 2006. 11777, 11786
- Bond, T. C., Habib, G. and Bergstrom, R. W.: Limitations in the enhancement of visible light absorption due to mixing state, *J. Geophys. Res.*, 111, D20211, doi:10.1029/2006JD007315, 2006. 11783
- Brock, C., Radke, L., and Hobbs, P.: Sulfur in particles in Arctic hazes derived from airborne in situ and lidar measurements, *J. Geophys. Res.*, 95(D13), 22369–22387, 1990. 11774
- Brock, C. A., Cozic, J., Bahreini, R., Froyd, K. D., Middlebrook, A. M., McComiskey, A., Brioude, J., Cooper, O. R., Stohl, A., Aikin, K. C., de Gouw, J. A., Fahey, D. W., Ferrare, R. A., Gao, R.-S., Gore, W., Holloway, J. S., Hübler, G., Jefferson, A., Lack, D. A., Lance, S., Moore, R. H., Murphy, D. M., Nenes, A., Novelli, P. C., Nowak, J. B., Ogren, J. A., Peischl, J., Pierce, R.

Physical and chemical properties of Arctic aerosols

B. Quennehen

Title Page

Abstract

Introduction

Conclusions

References

Tables

Figures

⏪

⏩

◀

▶

Back

Close

Full Screen / Esc

Printer-friendly Version

Interactive Discussion



Physical and chemical properties of Arctic aerosols

B. Quennehen

Title Page

Abstract

Introduction

Conclusions

References

Tables

Figures

◀

▶

◀

▶

Back

Close

Full Screen / Esc

Printer-friendly Version

Interactive Discussion



- B., Pilewskie, P., Quinn, P. K., Ryerson, T. B., Schmidt, K. S., Schwarz, J. P., Sodemann, H., Spackman, J. R., Stark, H., Thomson, D. S., Thornberry, T., Veres, P., Watts, L. A., Warneke, C., and Wollny, A. G.: Characteristics, sources, and transport of aerosols measured in spring 2008 during the aerosol, radiation, and cloud processes affecting Arctic Climate (ARCPAC) Project, *Atmos. Chem. Phys.*, 11, 2423–2453, doi:10.5194/acp-11-2423-2011, 2011. 11775
- 5 Browell, E., Butler, C., Kooi, S., Fenn, M., Harriss, R., and Gregory, G.: Large scale variability of ozone and aerosols in the summertime Arctic and sub-Arctic troposphere, *J. Geophys. Res.*, 97(D15), 16433–16450, 1992. 11774
- Canagaratna, M., Jayne, J., Jimenez, J., Allan, J., Alfarra, M., Zhang, Q., Onasch, T., Drewnick, F., Coe, H., Middlebrook, A., Delia, A., Williams, L., Trimborn, A., Northway, M., DeCarlo, P., Kolb, C., Davidovits, P., and Worsnop, D.: Chemical and microphysical characterization of ambient aerosols with the aerodyne aerosol mass spectrometer, *Mass Spectrom. Rev.*, 26(2), 185–222, 2007. 11777
- 10 Draxler, R. R. and Rolph, G. D.: HYSPLIT (HYbrid Single-Particle Lagrangian Integrated Trajectory) Model access via NOAA ARL READY Website, available at: <http://ready.arl.noaa.gov/HYSPLIT.php>, NOAA Air Resources Laboratory, Silver Spring, MD, 2010. 11784
- Dröeling, V. and Friederich, B.: Spatial distribution of the arctic haze aerosol size distribution in western and eastern Arctic, *Atmos. Res.*, 44(1–2), 133–152, 1997. 11774
- 15 Drewnick, F., Hings, S. S., DeCarlo, P., Jayne, J. T., Gonin, M., Fuhrer, K., Weimer, S., Jimenez, J. L., Demerjian, K. L., Borrmann, S., and Worsnop, D. R.: A New Time-of-Flight Aerosol Mass Spectrometer (TOF-AMS) –Instrument Description and First Field Deployment, *Aerosol Sci. Technol.*, 39(7), 637–658, 2005. 11777
- Eckhardt, S., Stohl, A., Beirle, S., Spichtinger, N., James, P., Forster, C., Junker, C., Wagner, T., Platt, U., and Jennings, S. G.: The North Atlantic Oscillation controls air pollution transport to the Arctic, *Atmos. Chem. Phys.*, 3, 1769–1778, doi:10.5194/acp-3-1769-2003, 2003. 11775
- 25 Fiebig, M., Stohl, A., Wendisch, M., Eckhardt, S., and Petzold, A.: Dependence of solar radiative forcing of forest fire aerosol on ageing and state of mixture, *Atmos. Chem. Phys.*, 3, 881–891, doi:10.5194/acp-3-881-2003, 2003. 11775, 11783, 11784, 11787, 11806
- Forster, C., Wandinger, U., Wotawa, G., James, P., Mattis, I., Althausen, D., Simmonds, P., O'Doherty, S., Jennings, S. G., Kleefeld, C., Schneider, J., Trickl, T., Kreipl, S., Jäger, H., and Stohl, A.: Transport of boreal forest fire emissions from Canada to Europe, *J. Geophys. Res.*, 106(D19), 22887–22906, 2001. 11778
- 30 Garrett, T. J. and Zhao, C.: Increased Arctic cloud longwave emissivity associated with pollution

Physical and chemical properties of Arctic aerosols

B. Quennehen

Title Page

Abstract

Introduction

Conclusions

References

Tables

Figures

◀

▶

◀

▶

Back

Close

Full Screen / Esc

Printer-friendly Version

Interactive Discussion



from mid-latitudes, *Nature*, 440, 787–789, 2006. 11774

Giglio, L., Descloitres, J., Justice, C. O., and Kaufman, Y.: An enhanced contextual fire detection algorithm for MODIS, *Remote Sens. Environ.*, 87(2–3), 273–282, 2003. 11780

Greenaway, K. R.: Experiences with Arctic flying weather, Royal Meteorol. Soc. Can., Branch, Toronto, Ont., Canada, 1950. 11774

Heald, C. L., Jacob, D. J., Alexander, B., Fairlie, T. D., Yantosca, R. M., and Chu, D. A.: Transpacific transport of Asian anthropogenic aerosols and its impact on surface air quality in the United States, *J. Geophys. Res.*, 111, D14310, doi:10.1029/2005JD006847, 2006. 11780

Hinds, W. C.: *Aerosol technology: properties, behaviour and measurement of airborne particles*, Wiley-Interscience, 1999. 11784

Hirdman, D., Sodemann, H., Eckhardt, S., Burkhardt, J. F., Jefferson, A., Mefford, T., Quinn, P. K., Sharma, S., Ström, J., and Stohl, A.: Source identification of short-lived air pollutants in the Arctic using statistical analysis of measurement data and particle dispersion model output, *Atmos. Chem. Phys.*, 10, 669–693, doi:10.5194/acp-10-669-2010, 2010. 11775

Honrath, R. E., Owen, R. C., Val Martin, M., Reid, J. S., Lapina, K., Fialho, P., Dziobak, M. P., Kleissl, J., and Westphal, D. L.: Regional and hemispheric impacts of anthropogenic and biomass burning emissions on summertime CO and O₃ in the North Atlantic lower free troposphere, *J. Geophys. Res.*, 109, D24310, doi:10.1029/2004JD005147, 2004. 11775

Hosseini, S., Li, Q., Cocker, D., Weise, D., Miller, A., Shrivastava, M., Miller, J. W., Mahalingam, S., Princevac, M., and Jung, H.: Particle size distributions from laboratory-scale biomass fires using fast response instruments, *Atmos. Chem. Phys.*, 10, 8065–8076, doi:10.5194/acp-10-8065-2010, 2010. 11783, 11784

Huang, L., Gong, S. L., Sharma, S., Lavoué, D., and Jia, C. Q.: A trajectory analysis of atmospheric transport of black carbon aerosols to Canadian high Arctic in winter and spring (1990–2005), *Atmos. Chem. Phys.*, 10, 5065–5073, doi:10.5194/acp-10-5065-2010, 2010. 11775

IPCC 2007: *Climate Change 2007: Synthesis Report*, in: *Contribution of Working groups I, II and III to the fourth Assessment Report of the Intergovernmental Panel on Climate Change*, edited by: Core Writing Team, Pachauri, R. K., and Reisinger, A., IPCC, Geneva, Switzerland, 2007. 11773, 11774

Iziomon, M. G., Lohmann, U., and Quinn, P. K.: 2006. Summertime pollution event in the Arctic and potential implications, *J. Geophys. Res.*, 111, D12206, doi:10.1029/2005JD006223, 2006. 11775

- Law, K. S., and Stohl, A.: Arctic Air Pollution: Origins and Impacts, *Science*, 315(5818), 1537–1540, 2007. 11774
- Lubin, D. and Vogelmann, A. M.: A climatologically significant aerosol longwave indirect effect in the Arctic, *Nature*, 439, 453–456, 2006. 11774
- 5 McConnell, J. R., Edwards, R., Kok, G. L., Flanner, M. G., Zender, C. S., Saltzman, E. S., Banta, J. R., Pasteris, D. R., Carter, M. M., and Kahl, J. D. W.: 20th-century industrial black carbon emissions altered Arctic climate forcing, *Science*, 317(5843), 1381–1384, 2007. 11775
- McNaughton, C. S., Clarke, A. D., Howell, S. G., Pinkerton, M., Anderson, B., Thornhill, L., Hudgins, C., Winstead, E., Dibb, J. E., Scheuer, E., and Maring, H.: Results from the DC-8 inlet characterization experiment (DICE): Airborne versus surface sampling of mineral dust and sea salt aerosols, *Aerosol Sci. Technol.*, 41, 136–159, 2007. 11776
- 10 Mitchell, J. M.: Visual range in the polar regions with particular reference to the Alaskan Arctic, *J. Atmos. Terr. Phys. Spec., Suppl.*, 195–211, 1957. 11774
- Nédélec, P., Cammas, J.-P., Thouret, V., Athier, G., Cousin, J.-M., Legrand, C., Abonnel, C., Lecoœur, F., Cayez, G., and Marizy, C.: An improved infrared carbon monoxide analyser for routine measurements aboard commercial Airbus aircraft: technical validation and first scientific results of the MOZAIC III programme, *Atmos. Chem. Phys.*, 3, 1551–1564, doi:10.5194/acp-3-1551-2003, 2003. 11778
- 15 Paris, J.-D., Stohl, A., Nédélec, P., Arshinov, M. Yu., Panchenko, M. V., Shmargunov, V. P., Law, K. S., Belan, B. D., and Ciais, P.: Wildfire smoke in the Siberian Arctic in summer: source characterization and plume evolution from airborne measurements, *Atmos. Chem. Phys.*, 9, 9315–9327, doi:10.5194/acp-9-9315-2009, 2009. 11775
- Paris, J.-D., Stohl, A., Ciais, P., Ndlec, P., Belan, B. D., Arshinov, M. Yu., and Ramonet, M.: Source-receptor relationships for airborne measurements of CO₂, CO and O₃ above Siberia: a cluster-based approach, *Atmos. Chem. Phys.*, 10, 1671–1687, doi:10.5194/acp-10-1671-2010, 2010. 11775
- 20 Petzold, A., Weinzierl, B., Huntrieser, H., Stohl, A., Real, E., Cozic, J., Fiebig, M., Hendricks, J., Lauer, A., Law, K., Roiger, A., Schlager, H., and Weingartner, E.: Perturbation of the European free troposphere aerosol by North American forest fire plumes during the ICARTT-ITOP experiment in summer 2004, *Atmos. Chem. Phys.*, 7, 5105–5127, doi:10.5194/acp-7-5105-2007, 2007. 11775, 11783, 11784, 11787, 11806
- 25 Quinn, P. K., Miller, T. L., Bates, T. S., Ogren, J. A., Andrews, E., and Shaw, G. E.: A three-year record of simultaneously measured aerosol chemical and optical properties at Barrow,

**Physical and
chemical properties
of Arctic aerosols**

B. Quennehen

Title Page

Abstract

Introduction

Conclusions

References

Tables

Figures

◀

▶

◀

▶

Back

Close

Full Screen / Esc

Printer-friendly Version

Interactive Discussion



Physical and chemical properties of Arctic aerosols

B. Quennehen

Title Page

Abstract

Introduction

Conclusions

References

Tables

Figures

◀

▶

◀

▶

Back

Close

Full Screen / Esc

Printer-friendly Version

Interactive Discussion



- Alaska, *J. Geophys. Res.*, 107(D11), 4130, doi:10.1029/2001JD001248, 2002. 11774
- Quinn, P. K., Andrews, B., Christensen, J., Dutton, E., and Shaw, G.: Acidifying pollutants, Arctic haze, and acidification in the Arctic, *Arctic Research of the United States*, 19, 26–33, 2005. 11776
- 5 Quinn, P. K., Shaw, G., Andrews, E., Dutton, E. G., Ruoho-Airola, T., and Gong, S. L.: Arctic Haze: Current trend and knowledge gaps, *Tellus B*, 59(1), 99–114, 2007. 11774, 11775
- Quinn, P. K., Bates, T. S., Baum, E., Doubleday, N., Fiore, A. M., Flanner, M., Fridlind, A., Garrett, T. J., Koch, D., Menon, S., Shindell, D., Stohl, A., and Warren, S. G.: Short-lived pollutants in the Arctic: their climate impact and possible mitigation strategies, *Atmos. Chem. Phys.*, 8, 1723–1735, doi:10.5194/acp-8-1723-2008, 2008. 11774
- 10 Real, E., Law, K. S., Weinzierl, B., Fiebig, M., Petzold, A., Wild, O., Methven, J., Arnold, S., Stohl, A., Huntrieser, H., Roiger, A., Schlager, H., Stewart, D., Avery, M., Sachse, G., Browell, E., Ferrare, R., and Blake, D.: Processes influencing ozone levels in Alaskan forest fire plumes during long-range transport over the North Atlantic, *J. Geophys. Res.*, 112, D10S41, doi:10.1029/2006JD007576, 2007. 11781
- 15 Reid, J. S., Hobbs, P. V., Ferek, R. J., Blake, D. R., Martins, J. V., Dunlap, M. R., and Liousse, C.: Physical, chemical, and optical properties of regional hazes dominated by smoke in Brazil, *J. Geophys. Res.*, 103(D24), 32059–32080, 1998. 11783
- Reid, J. S., Koppmann, R., Eck, T. F., and Eleuterio, D. P.: A review of biomass burning emissions part II: intensive physical properties of biomass burning particles, *Atmos. Chem. Phys.*, 5, 799–825, doi:10.5194/acp-5-799-2005, 2005. 11774
- 20 Ricard, V., Jaffrezo, J., Kerminen, V., Hillamo, R. E., Sillanpaa, M., Ruellan, S., Liousse, C., and Cachier, H.: Two years of continuous aerosol measurements in northern Finland, *J. Geophys. Res.*, 107(D11), 4129, doi:10.1029/2001JD000952, 2002. 11774
- 25 Rolph, G. D.: Real-time Environmental Applications and Display sYstem (READY) Website, available at: <http://ready.arl.noaa.gov>, NOAA Air Resources Laboratory, Silver Spring, MD, 2010. 11784
- Schmale, J., Schneider, J., Jurkat, T., Voigt, C., Kalesse, H., Rautenhaus, M., Lichtenstern, M., Schlager, H., Ancellet, G., Arnold, F., Gerding, M., Mattis, I., Wendisch, M., and Borrmann, S.: Aerosol layers from the 2008 eruptions of Mount Okmok and Mount Kasatochi: In situ upper troposphere and lower stratosphere measurements of sulfate and organics over Europe, *J. Geophys. Res.*, 115, D00L07, doi:10.1029/2009JD013628, 2010. 11777, 11778
- 30 Schmale, J., Schneider, J., Ancellet, G., Quennehen, B., Stohl, A., Sodemann, H., Burkhardt, J.,

**Physical and
chemical properties
of Arctic aerosols**

B. Quennehen

Title Page

Abstract

Introduction

Conclusions

References

Tables

Figures

◀

▶

◀

▶

Back

Close

Full Screen / Esc

Printer-friendly Version

Interactive Discussion



- Hamburger, T., Arnold, S. R., Schwarzenboeck, A., Borrmann, S., and Law, K. S.: Source identification and airborne chemical characterisation of aerosol pollution from long-range transport over Greenland during POLARCAT summer campaign 2008, *Atmos. Chem. Phys. Discuss.*, 11, 7593–7658, doi:10.5194/acpd-11-7593-2011, 2011. 11780, 11782
- 5 Schwarz, J. P., Gao, R. S., R., Spackman J., Watts, L. A., Thomson, D. S, Fahey, D.W, Ryerson, T. B., Peischl, J., Holloway, J. S., Trainer, M., Baynard, T., Lack, D. A., De Gouw, J. A., Warneke, C., and Del Negro, L. A.: Measurement of the mixing state, mass, and optical size of individual black carbon particles in urban and biomass burning emissions, *J. Geophys. Res.*, 35(13), L13810, doi:10.1029/2008GL033968, 2008. 11783
- 10 Sharma, S., Brook, J. R., Cachier, H., Chow, J., Gaudenzi, A., and Lu, G.: Light absorption and thermal measurements of black carbon in different regions of Canada, *J. Geophys. Res.*, 107(D24), 4771, doi:10.1029/2002JD002496, 2002. 11778, 11786
- Sharma, S., Lavoué, D., Cachier, H., Barrie, L. A., and Gong, S. L.: Long-term trends of black carbon concentrations in the Canadian Arctic, *J. Geophys. Res.*, 109, D15203, doi:10.1029/2003JD004331, 2004. 11775
- 15 Sharma, S., Andrews, E., Barrie, L. A., Ogren, J. A., and Lavoué, D.: Variations and sources of the equivalent black carbon in the high Arctic revealed by long-term observations at Alert and Barrow 1989–2003, *J. Geophys. Res.*, 111, D14208, doi:10.1029/2005JD006581, 2006. 11775
- 20 Shaw, G. E.: The vertical distribution of atmospheric aerosols at Barrow, Alaska, *Tellus*, 27, 39–50, 1975. 11774
- Singh, H. B., Anderson, B. E., Brune, W. H., Cai, C., Cohen, R. C., Crawford, J. H., Cubison, M. J., Czech, E. P., Emmons, L., Fuelberg, H. E., Huey, G., Jacob, D. J., Jimenez, J. L., Kaduwela, A., Kondo, Y., Mao, J., Olson, J. R., Sachse, G. W., Vay, S. A., Weinheimer, A.,
25 Wennberg, P. O., and Wisthaler, A.: Pollution influence on atmospheric composition and chemistry at high northern latitudes: Boreal and California forest fire emissions, *Atmos. Environ.*, 44(36), 4553–4564, 2010. 11780
- Sirois, A. and Barrie, L.: Arctic lower tropospheric aerosol trends and composition at Alert, Canada: 1980–1995, *J. Geophys. Res.*, 104(D9), 11599–11618, 1999. 11774
- 30 Springston, S. R. and Sedlacek III, A. J.: Noise characteristics of an instrumental particle absorbance technique, *Aerosol Sci. Technol.*, 41, 1110–1116, 2007. 11778
- Stohl, A.: Characteristics of atmospheric transport into the Arctic troposphere, *J. Geophys. Res.*, 111, 0148–0227, 2006. 11775

**Physical and
chemical properties
of Arctic aerosols**

B. Quennehen

Title Page

Abstract

Introduction

Conclusions

References

Tables

Figures

◀

▶

◀

▶

Back

Close

Full Screen / Esc

Printer-friendly Version

Interactive Discussion



Stohl, A., Hittenberger, M., and Wotawa, G.: Validation of the lagrangian particle dispersion model FLEXPART against large-scale tracer experiment data, *Atmos. Environ.*, 32(24), 4245–4264, 1998. 11779

Stohl, A., Forster, C., Frank, A., Seibert, P., and Wotawa, G.: Technical note: The Lagrangian particle dispersion model FLEXPART version 6.2, *Atmos. Chem. Phys.*, 5, 2461–2474, doi:10.5194/acp-5-2461-2005, 2005. 11779, 11782

Stohl, A., Andrews, E., Burkhardt, J. F., Forster, C., Herber, A., Hoch, S. W., Kowal, D., Lunder, C., Mefford, T., Ogren, J. A., Sharma, S., Spichtinger, N., Stebel, K., Stone, R., Strm, J., Trseth, K., Wehrli, C., and Yttri, K. E.: Pan-Arctic enhancements of light absorbing aerosol concentrations due to North American boreal forest fires during summer 2004, *J. Geophys. Res.*, 111, 0148–0227, 2006. 11775

Stohl, A., Berg, T., Burkhardt, J. F., Fjæraa, A. M., Forster, C., Herber, A., Hov, Ø., Lunder, C., McMillan, W. W., Oltmans, S., Shiobara, M., Simpson, D., Solberg, S., Stebel, K., Strm, J., Tørseth, K., Treffeisen, R., Virkkunen, K., and Yttri, K. E.: Arctic smoke - record high air pollution levels in the European Arctic due to agricultural fires in Eastern Europe in spring 2006, *Atmos. Chem. Phys.*, 7, 511–534, doi:10.5194/acp-7-511-2007, 2007. 11775, 11782

Stohl, A., Forster, C., Eckhardt, S., Spichtinger, N., Huntrieser, H., Heland, J., Schlager, H., Wilhelm, F., Arnold, F., and Cooper, O.: backward modeling study of intercontinental pollution transport using aircraft measurements, *J. Geophys. Res.*, 108, 4370, doi:10.1029/2002JD002862, 2009. 11779

Twomey, S.: The Influence of Pollution on the Shortwave Albedo of Clouds, *J. Atmos. Sci.*, 34(7), 1149–1152, 1977. 11774

Villani, P., Picard, D., Michaud, V., Laj, P., and Wiedensohler, A.: Design and Validation of a Volatility Hygroscopic Tandem Differential Mobility Analyzer (VH-TDMA) to Characterize the Relationships Between the Thermal and Hygroscopic Properties of Atmospheric Aerosol Particles, *Aerosol Sci. Technol.*, 42(9), 729–741, 2008. 11776

Physical and chemical properties of Arctic aerosols

B. Quennehen

Table 1. Log-normally fitted size distribution parameters for the 16 selected time windows.

Flight date	Origin	Aitken mode			Intermediate mode			Accumulation mode			Coarse mode		
		$n_1(\text{cm}^{-3})$	σ_1	$d_{m1}(\text{nm})$	$n_2(\text{cm}^{-3})$	σ_2	$d_{m2}(\text{nm})$	$n_3(\text{cm}^{-3})$	σ_3	$d_{m3}(\text{nm})$	$n_4(\text{cm}^{-3})$	σ_4	$d_{m4}(\text{nm})$
8 July	Can. BF	125.46	1.29	41.79	173.57	1.77	75.39	65.37	1.42	229.60	2.54	1.89	535.89
	Can. BF	365.98	1.36	39.87	165.94	1.80	109.15	15.13	1.30	179.86	0.09	1.60	783.201
	Can. BF	150.60	1.25	32.62	141.42	1.44	65.00	101.46	1.51	187.98	3.55	1.12	535.12
	Anth. NA	16.57	1.18	30.59	199.08	1.80	65.36	139.25	1.62	150.00	0.11	1.58	3000.00
12 July	Can. BF	107.49	1.35	44.43	58.22	1.73	86.00	1.74	1.30	441.09	0.06	1.25	1957.43
	Can. BF	415.44	1.38	52.31	21.60	1.32	128.38	24.21	1.73	155.84	0.13	1.54	2224.18
	Can. BF	31.21	1.31	40.41	83.35	1.72	96.41	0.00	1.34	1200.00	0.13	1.33	1420.79
	Can. BF	66.84	1.25	39.55	106.83	1.43	66.49	85.32	1.58	150.00	2.35	1.29	500.00
	Can. BF	160.84	1.38	46.40	126.45	1.77	116.48	0.25	1.30	549.87	0.17	1.46	1385.80
	Can. BF	62.61	1.28	40.65	130.84	1.53	66.29	63.08	1.62	150.00	1.10	1.55	500.00
13 July	Can. BF	62.49	1.28	35.79	199.25	1.80	89.82	29.48	1.33	312.96	0.14	1.60	318.541
	Can. BF	195.15	1.63	51.10	87.00	1.63	150.22	8.39	1.30	378.62	0.15	1.41	1500.42
14 July	Anth. NA	159.82	1.80	61.44	39.30	1.30	160.16	16.44	1.30	296.60	2.12	1.54	500.13
	Alk. AK	26.12	1.10	32.60	306.11	1.80	68.23	97.34	1.48	150.00	0.37	1.82	3000.00
	Alk. AK	373.65	1.80	69.10	35.39	1.38	200.00	1.07	1.80	1200.00	2.54	1.21	3000.00
	Alk. AK	4.05	1.17	33.76	113.66	1.53	66.92	42.05	1.58	157.12	0.15	1.84	1407.96

Title Page

Abstract

Introduction

Conclusions

References

Tables

Figures

◀

▶

◀

▶

Back

Close

Full Screen / Esc

Printer-friendly Version

Interactive Discussion



Physical and chemical properties of Arctic aerosols

B. Quennehen

Table 2. Volume concentrations for BC (V_{psap}) calculated from PSAP absorption measurements and for Aitken mode particles (V_{Aitken}) derived from fitted size distributions (Table 1) for the 11 Canadian boreal forest fires events. Ratios of both volumes are added in the fourth column. In addition, ΔCO mean concentration are presented as well as the mean FLEXPART fire tracer age.

Flight date	NA period number	V_{psap} ($\text{mm}^3 \text{m}^{-3}$)	V_{Aitken} ($\text{mm}^3 \text{m}^{-3}$)	$100 \cdot V_{\text{psap}}/V_{\text{Aitken}}$ (%)	ΔCO (ppbv)	Mean Flexpart age (days)
8 July	1	3.355×10^{-6}	1.605×10^{-5}	20.9	35.0	11.4
	2	1.491×10^{-5}	2.357×10^{-5}	63.3	68.4	6.4
	3	7.865×10^{-6}	1.527×10^{-5}	51.5	70.4	8.2
12 July	1	8.285×10^{-6}	9.557×10^{-6}	86.7	38.8	11.7
	2	1.685×10^{-5}	3.332×10^{-5}	50.6	27.8	11.6
	3	9.587×10^{-7}	5.378×10^{-6}	17.8	41.8	12.4
	4	1.153×10^{-5}	1.183×10^{-5}	97.5	20.4	12.0
	5	1.189×10^{-5}	1.502×10^{-5}	79.2	34.5	12.1
	6	8.902×10^{-6}	1.266×10^{-5}	70.3	32.8	11.9
13 July	1	Not av.	1.170×10^{-5}	Not av.	24.7	13.0
	2	1.534×10^{-5}	1.377×10^{-5}	111.4	38.6	13.4

[Title Page](#)
[Abstract](#)
[Introduction](#)
[Conclusions](#)
[References](#)
[Tables](#)
[Figures](#)
[Back](#)
[Close](#)
[Full Screen / Esc](#)
[Printer-friendly Version](#)
[Interactive Discussion](#)


**Physical and
chemical properties
of Arctic aerosols**

B. Quennehen

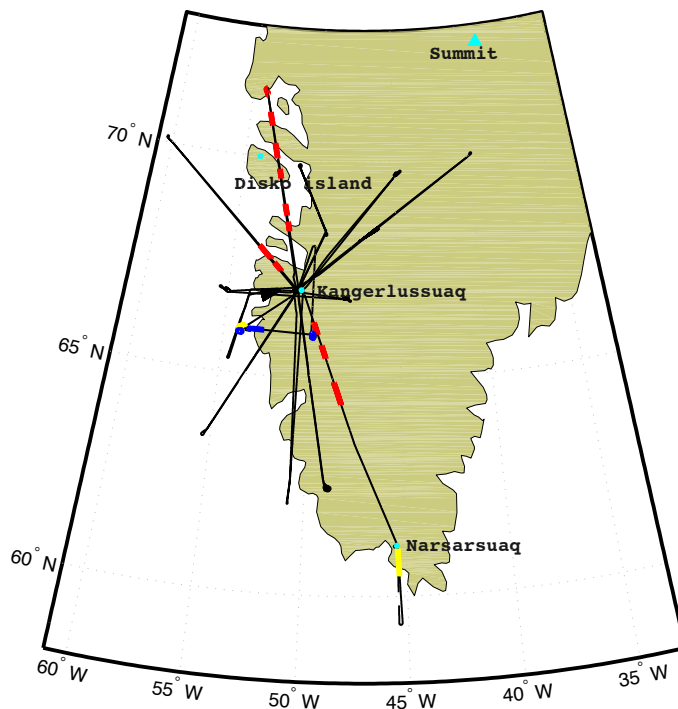


Fig. 1. ATR-42 flight trajectories during the POLARCAT-France summer campaign. Flight segments related to air mass origins from the North American continent studied in this paper are highlighted in red and blue for Canadian and Alaskan forest fires and in yellow for anthropogenic air masses.

Title Page

Abstract

Introduction

Conclusions

References

Tables

Figures

◀

▶

◀

▶

Back

Close

Full Screen / Esc

Printer-friendly Version

Interactive Discussion



Physical and chemical properties of Arctic aerosols

B. Quennehen

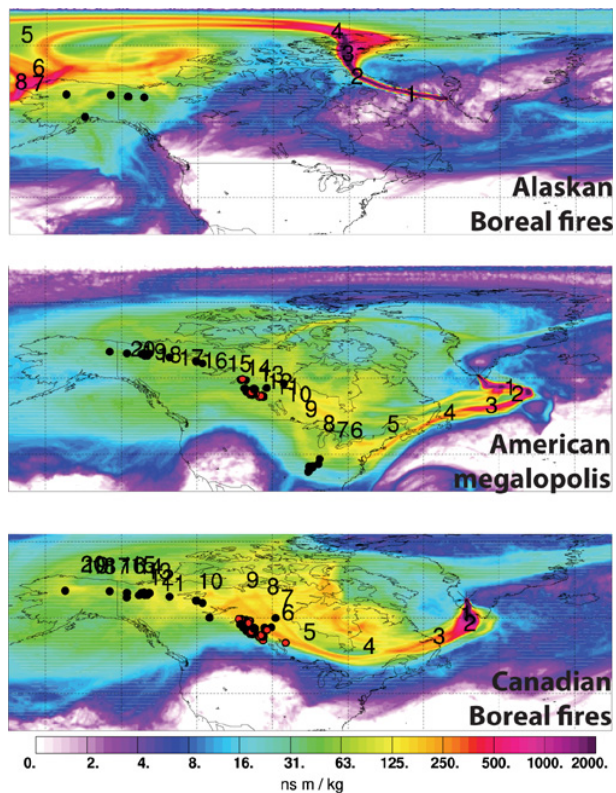


Fig. 2. FLEXPART North American column-integrated potential emissions sensitivities (PES).

Title Page

Abstract Introduction

Conclusions References

Tables Figures

◀ ▶

◀ ▶

Back Close

Full Screen / Esc

Printer-friendly Version

Interactive Discussion



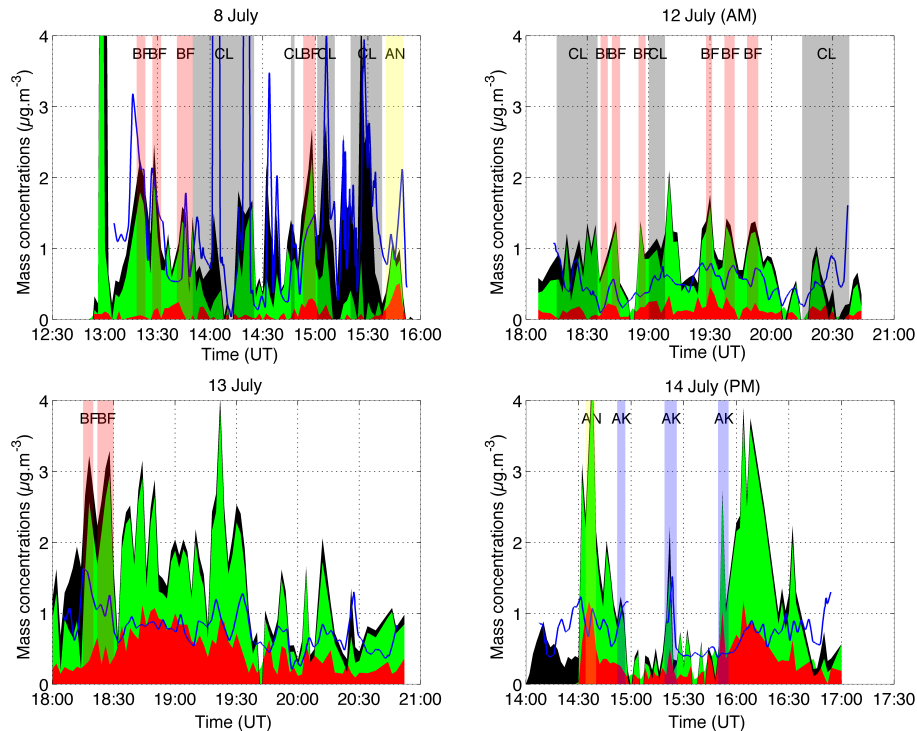


Fig. 3. Stacked aerosol mass concentrations in $\mu\text{g m}^{-3}$ for sulphate (red), organics (green), and refractory material (black). Air mass origins determined with FLEXPART integrated-column PES are noted with AN for North-American megalopolis, AK for Alaska, BF for Canadian boreal forest fires while cloud presence is indicated with “CL”. The blue line represents the estimated mass of particulate material at ambient temperature calculated from SMPS aerosol size distributions.

Physical and chemical properties of Arctic aerosols

B. Quennehen

Title Page

Abstract Introduction

Conclusions References

Tables Figures

◀ ▶

◀ ▶

Back Close

Full Screen / Esc

Printer-friendly Version

Interactive Discussion



Physical and chemical properties of Arctic aerosols

B. Quennehen

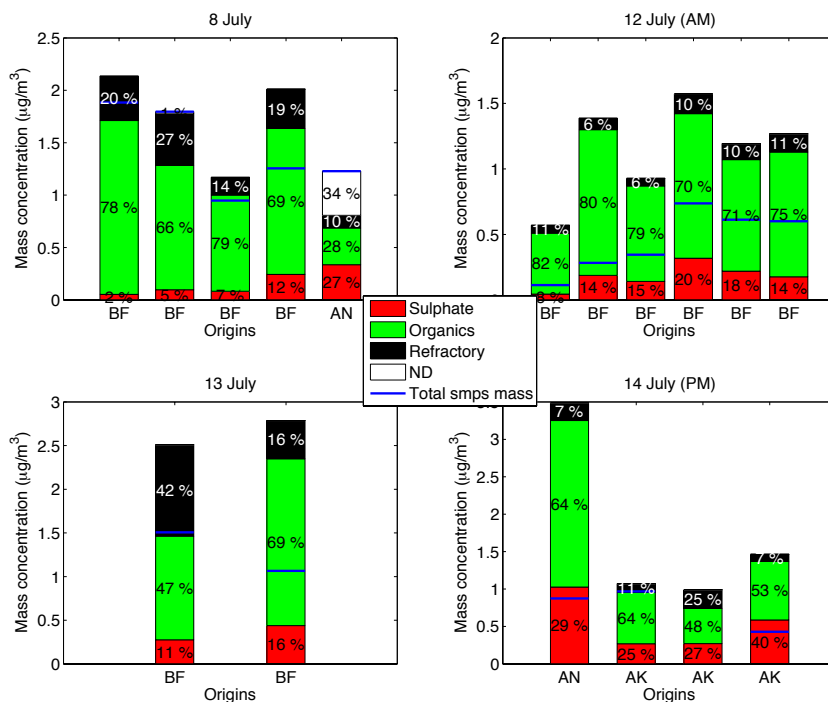


Fig. 4. Aerosol chemical composition for the selected time windows. Blue line indicate the mass of aerosol at ambient temperature, determined with the SMPS data. Red, green, black and white colours are for sulphate, organics, refractory and not determined part (ND), respectively (Air mass origins determined with Flexpart integrated-column PES are noted with AN for North American megalopolis and AK and BF for Alaskan and Canadian boreal forest fires).

Title Page

Abstract

Introduction

Conclusions

References

Tables

Figures

◀

▶

◀

▶

Back

Close

Full Screen / Esc

Printer-friendly Version

Interactive Discussion



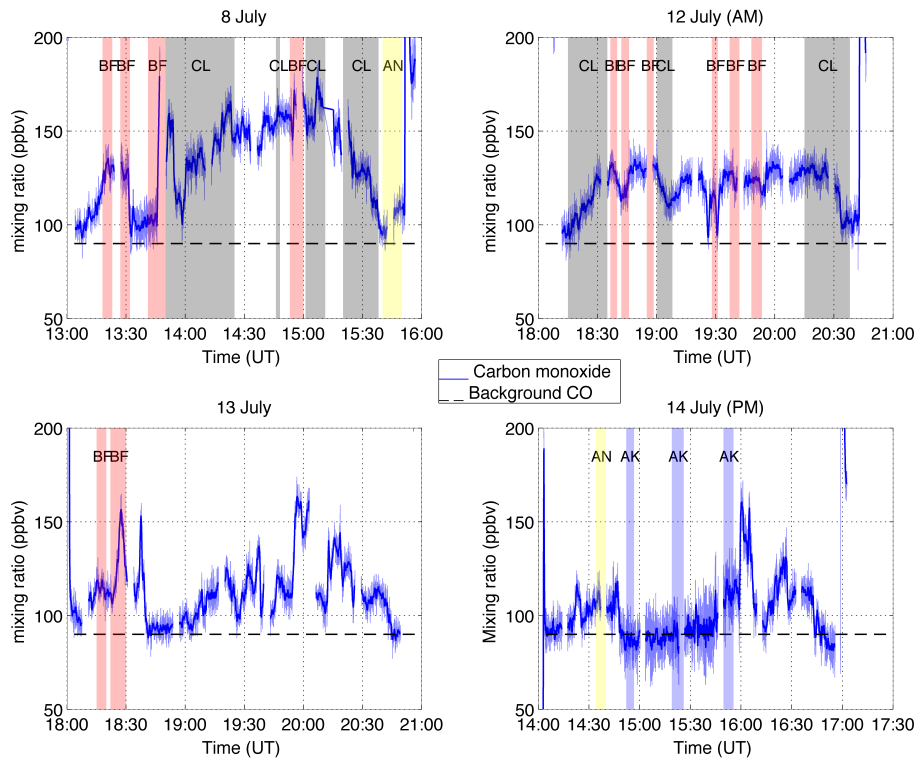


Fig. 5. Time series of ATR-42 in-situ measurements of carbon monoxide (CO, in blue) mixing ratios (in ppbv) along the flight tracks. A value of background CO equal to 90 ppbv is indicated with the black dashed line. Air masses originating from North-America are highlighted (as in Fig. 3).

**Physical and
chemical properties
of Arctic aerosols**

B. Quennehen

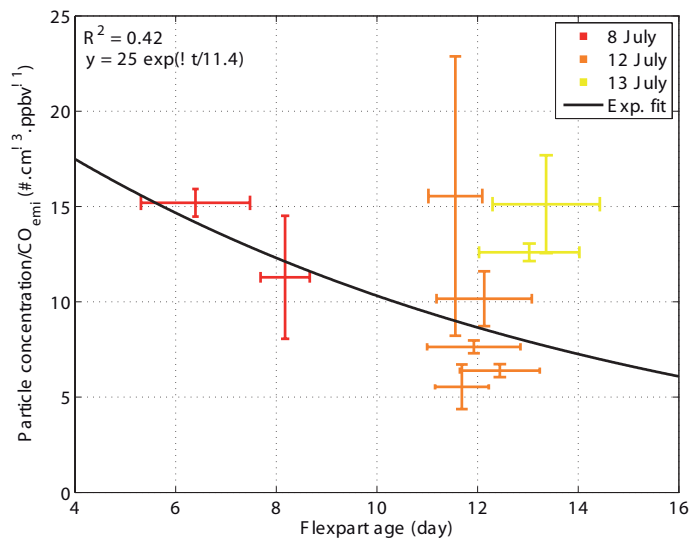


Fig. 6a. Mean aerosol particle concentrations (in # cm⁻³, for diameters < 500 nm) normalised with FLEXPART CO emission estimations as a function of the mean FLEXPART age in days for the Canadian boreal fire plumes. The corresponding data points are colour coded with respect to flight numbers. An exponential fit of all data points is plotted in black.

Title Page

Abstract

Introduction

Conclusions

References

Tables

Figures

◀

▶

◀

▶

Back

Close

Full Screen / Esc

Printer-friendly Version

Interactive Discussion



Physical and chemical properties of Arctic aerosols

B. Quennehen

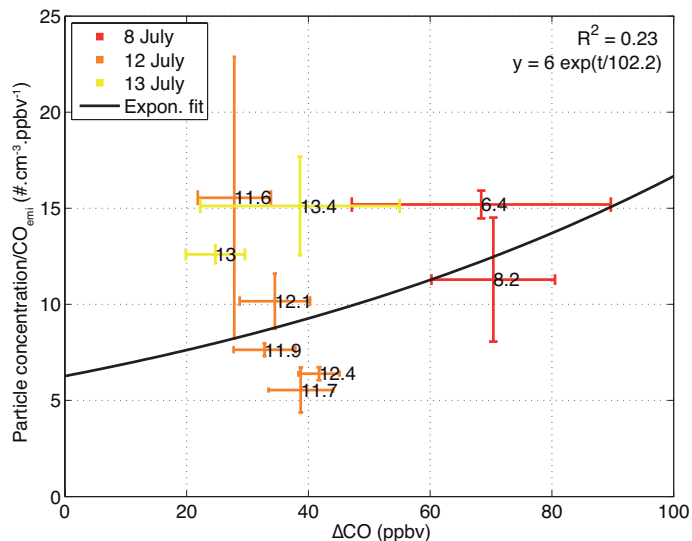


Fig. 6b. Mean aerosol particle concentrations (in $\# \text{ cm}^{-3}$, for diameters $< 500 \text{ nm}$) normalised with FLEXPART CO emission estimations as a function of the mean CO enhancements in ppbv for the Canadian boreal fire plumes. The corresponding data points are colour coded with respect to flight numbers, the mean FLEXPART age is added in black. An exponential fit of all data points is plotted in black.

[Title Page](#)
[Abstract](#)
[Introduction](#)
[Conclusions](#)
[References](#)
[Tables](#)
[Figures](#)
[◀](#)
[▶](#)
[◀](#)
[▶](#)
[Back](#)
[Close](#)
[Full Screen / Esc](#)
[Printer-friendly Version](#)
[Interactive Discussion](#)


Physical and chemical properties of Arctic aerosols

B. Quennehen

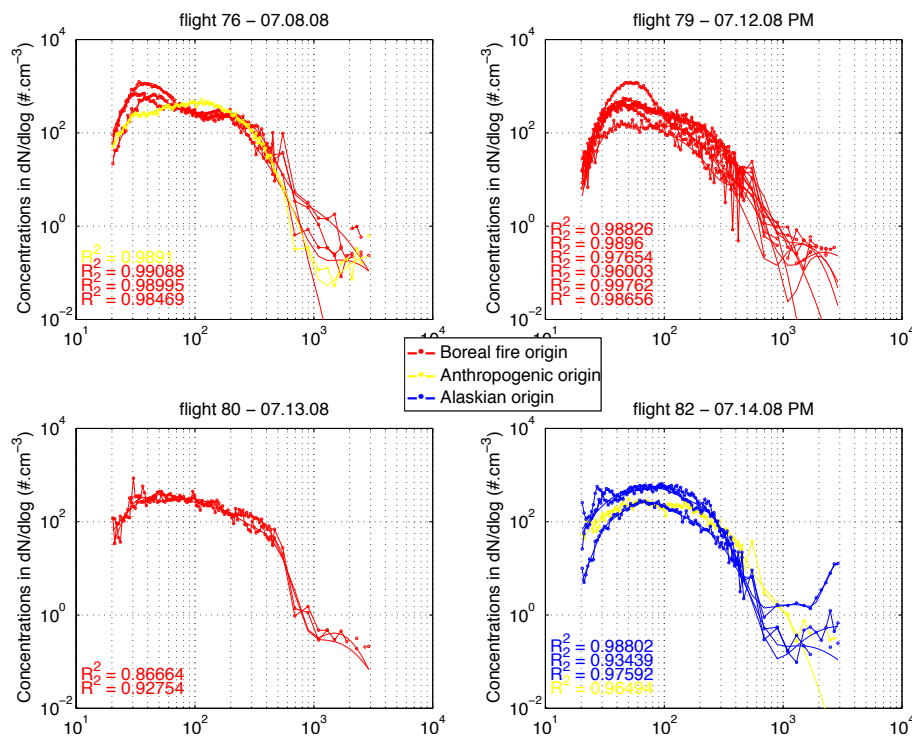


Fig. 7. Log-normal fitted aerosol size distributions (solid line) and raw measurements (solid line with symbol) for the selected time windows of the 4 respective flights.

Title Page

Abstract

Introduction

Conclusions

References

Tables

Figures

◀

▶

◀

▶

Back

Close

Full Screen / Esc

Printer-friendly Version

Interactive Discussion



**Physical and
chemical properties
of Arctic aerosols**

B. Quennehen

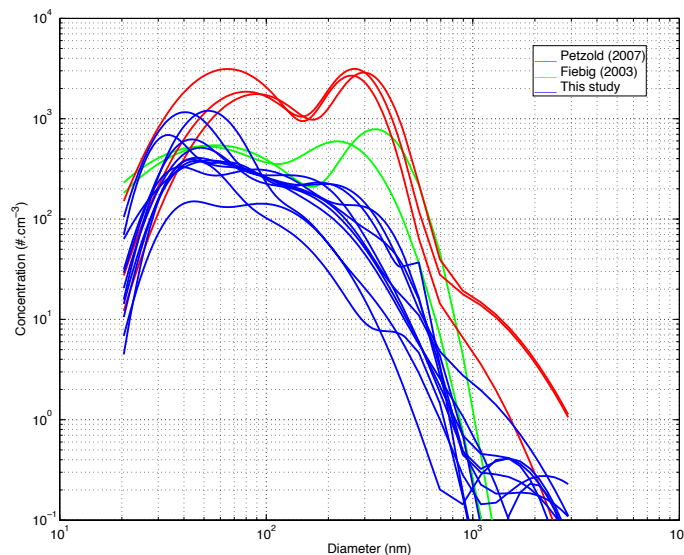


Fig. 8. Fitted aerosol size distributions of air masses originating from North-American boreal forest fires measured over Central Europe (Petzold et al., 2007) in solid red line, Germany (Fiebig et al., 2003) in solid green line, and Greenland (this study) in solid blue line.

[Title Page](#)[Abstract](#)[Introduction](#)[Conclusions](#)[References](#)[Tables](#)[Figures](#)[◀](#)[▶](#)[◀](#)[▶](#)[Back](#)[Close](#)[Full Screen / Esc](#)[Printer-friendly Version](#)[Interactive Discussion](#)

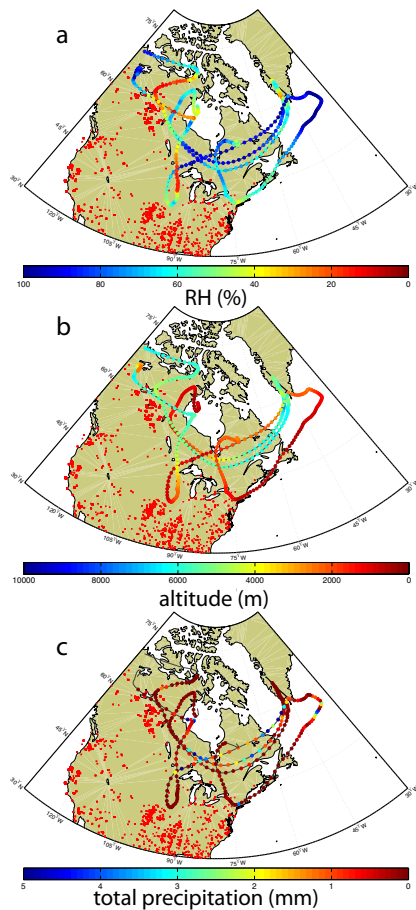


Fig. 9. HYSPLIT back-trajectories for the four forest fire time windows on 8 July. (a) Relative humidity (RH), (b) altitude and (c) total precipitation are colour coded along the back-trajectories. Red dots symbolize fire spots from MODIS.

Physical and chemical properties of Arctic aerosols

B. Quennehen

Title Page

Abstract Introduction

Conclusions References

Tables Figures

◀ ▶

◀ ▶

Back Close

Full Screen / Esc

Printer-friendly Version

Interactive Discussion



Physical and chemical properties of Arctic aerosols

B. Quennehen

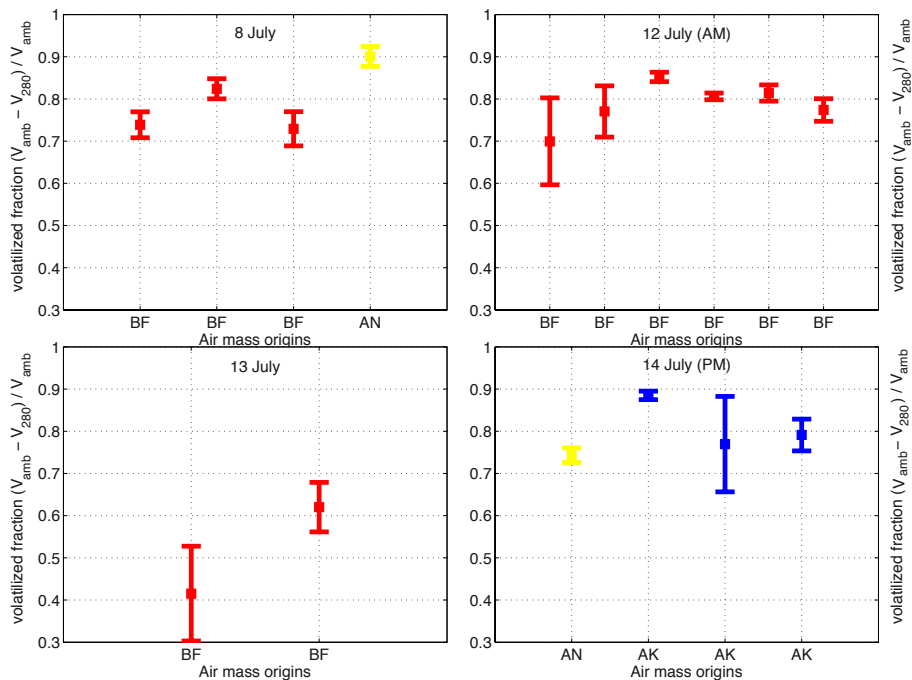


Fig. 10. Mean aerosol volatile volume fractions including standard deviations for the selected time windows of the 4 flights.

Title Page

Abstract

Introduction

Conclusions

References

Tables

Figures

◀

▶

◀

▶

Back

Close

Full Screen / Esc

Printer-friendly Version

Interactive Discussion

